Interaction of synthetic peptides corresponding to the scaffolding domain of Caveolin-3 with model membranes

ARTICLE *in* BIOPOLYMERS · JANUARY 2006

Impact Factor: 2.39 · DOI: 10.1002/bip.20595 · Source: PubMed

3 AUTHORS, INCLUDING:

Medicharla Venkata Jagannadham
Centre for Cellular and Molecular Biology
50 PUBLICATIONS **846** CITATIONS
SEE PROFILE

Ram Nagaraj
Centre for Cellular and Molecular Biology
174 PUBLICATIONS **3,657** CITATIONS
SEE PROFILE

Bekshe L. Sowmya
M. V. Jagannadham
Ramakrishnan Nagaraj
Centre for Cellular and Molecular Biology, Uppal Road, Hyderabad 500 007, India

Interaction of Synthetic Peptides Corresponding to the Scaffolding Domain of Caveolin-3 with Model Membranes

Received 14 June 2006; revised 21 August 2006; accepted 27 August 2006
Published online 31 August 2006 in Wiley InterScience (www.interscience.wiley.com). DOI 10.1002/bip.20595

Abstract: *Caveolin-1 and -3 are among the few proteins in which the functional domains are contiguous and modular. The interaction of synthetic peptides spanning the scaffolding domain of caveolin-3 with model membranes has been investigated. The peptides include the scaffolding domain, the aromatic and positively charged residues at the C-terminal end of this domain as well as deletion of three amino acids TFT, observed in certain patients with limb girdle muscular dystrophy. All of the peptides appear to be peripherally bound to the bilayer surface. However, no preferential binding to sphingomyelin and cholesterol-containing lipid vesicles was observed. Deletion of TFT appears to affect the association with lipid vesicles compared with the native sequence. Association with lipids decreases considerably when TFT as well as the aromatic-rich segment YWFYR, which occurs at the extreme C-terminus of the scaffolding domain, are deleted.* © 2006 Wiley Periodicals, Inc. Biopolymers (Pept Sci) 84: 615–624, 2006

This article was originally published online as an accepted preprint. The "Published Online" date corresponds to the preprint version. You can request a copy of the preprint by emailing the Biopolymers editorial office at biopolymers@wiley.com

Keywords: *caveolin scaffolding domain; membrane binding; synthetic peptides; model membranes; fluorescence spectroscopy; membrane surface*

INTRODUCTION

Caveolae are flask-shaped invaginations of the plasma membrane, which are 50 to 100 nm in diameter.[1,2] These dynamic structures can vary in shape and are found in various cell types. They are abundant in endothelial cells, adipocytes, fibroblasts, myocytes, pneumocytes, and epithelial cells.[3–9] Both single and multiple clusters of caveolae are observed in cells. Caveolae are enriched in sphingolipids and cholesterol, which render them resistant to detergent solubilization by Triton X-100. Caveolae are increasingly recognized to participate in various cellular processes such as endocytosis, cholesterol and lipid homeostasis, and signal transduction pathway regulation.[3–9]

The principal proteins found in caveolae are caveolins.[10–14] Among the three caveolins, caveolin-1 and caveolin-2 have nearly identical tissue distribution[7,15,16] whereas caveolin-3 is specific to muscle cells.[5,7,17,18] Caveolin-1 forms homo-oligomers composed of 14 to 16 monomers and migrates as a high molecular mass complex in velocity gradient centrifugation.[19,20] Caveolin-1 and -2 are coexpressed and form hetero-oligomers.[16]

Correspondence to: R. Nagaraj; e-mail: nraj@ccmb.res.in
Biopolymers (Peptide Science), Vol. 84, 615–624 (2006)

Table I Sequences of Caveolin Scaffolding Domain of Caveolin-3 and Synthetic Peptides

Caveolin-3	D G V W K V S Y T T F T V S K Y W C Y R
Synthetic Peptides	
CSD AR	K Y W F Y R
CSD19	D G V W K V S Y T T F T V S K Y W F Y
CSD16[a]	D G V W K V S Y T * * * V S K Y W F Y
CSD15-AR	D G V W K V S Y T T F T V S K
CSD12-AR[a]	D G V W K V S Y T * * * V S K

[a] *** Denotes deletion of TFT.

Various discrete structural and functional domains in caveolins 1–3 have been identified.[21–26] A hydrophobic segment spanning residues 102–134 in caveolin-1 directs the membrane topology wherein both the amino and carboxyl termini are directed toward cytoplasm.[19,27] The segment of caveolin-1 spanning residues 82–101 regulates the activity of signaling molecules[13] and has been termed the Caveolin Scaffolding Domain (CSD).[22,24] This segment alone is sufficient for membrane attachment of "passenger" proteins and contributes to membrane attachment of caveolin-1.[22,24] Further, molecular dissection of the CSD has revealed that the sequence KYWFYR, which occurs at the C-terminal end of the CSD of caveolin-1, has membrane attachment properties as inferred from its ability to target GFP to caveolae.[26]

Mutations in the gene coding for human caveolin-3 have been identified in human limb girdle muscular dystrophy.[28,29] A deletion resulting in the loss of the three amino acids TFT within the CSD was identified. This deletion resulted in increased Triton X-100 solubility of membrane-bound caveolin-3, formation of unstable high molecular mass oligomers,[29] and retention in Golgi membranes.[30] Deletion of TFT also caused considerably reduced localization of the protein to the plasma membrane and to lipid rafts.[31,32]

We have investigated how synthetic peptides corresponding to CSD of caveolin-3 and the CSD variant in which TFT has been deleted interact with model membranes. We have also investigated the membrane-binding ability of the sequence KYWFYR that occurs at the C-terminal end of CSD and the effects of deleting this sequence from the peptides corresponding to CSD with and without TFT deletion. The sequences are shown in Table I.

MATERIALS AND METHODS

Materials

9-Fluorenylmethoxycarbonyl (F-moc) amino acids were purchased from Novabiochem AG (Merck Biosciences AG, Laufelfingen, Switzerland) and Advanced Chemtech (Louisville, KY, USA). Other reagents used for peptide synthesis included *N*-hydroxybenzotriazole hydrate (HOBT, Advanced Chemtech), 2-(1*H*- benzotriazol-1-yl)-1,1,3,3-tetramethyluronium hexaflurophosphate (HBTU, Advanced Chemtech), *N*,*N*-diisopropylethylamine (DIEA, Sigma) and dimethylformamide (DMF, Spectrochem, Mumbai, India). Phospholipids 1-palmitoyl-2-oleoyl-phosphatidylcholine (PC), 1-palmitoyl-2-oleoyl-phosphatidylglycerol (PG), and sphingomyelin (SM) were purchased from Avanti Polar Lipids (Alabaster, AL, USA). 5-(Dimethylamino) naphthalene-1-sulfonyl-L-α-phosphatidylethanolamine (DNS-PE) was purchased from Molecular Probes (Eugene, OR, USA). D_2O and cholesterol (CHL) were obtained from Sigma–Aldrich (St. Louis, MO, USA). All other chemicals used were of highest grade available.

Peptide Synthesis and Purification

All of the peptides were synthesized by solid-phase methods using F-moc chemistry.[33] Peptide resins were treated with reagent K[34] containing vol/vol of 82.5% TFA, 5% water, 5% phenol, 5% thioanisole, and 2.5% ethanedithiol to cleave the peptide from the resin and to remove the side chain–protecting groups. Peptide purification was accomplished on a Hewlett Packard 1100 series HPLC instrument (Palo Alto, CA, USA) on a reversed phase C_{18} BioRad column (Biorad, Hercules, CA, USA). The peptides were further characterized by matrix assisted laser desorption/ionization time-of-flight (MALDI–TOF) mass spectrometry on a Voyager DE STR mass spectrometer (PerSeptive Biosystems, Foster City, CA, USA) using recrystallized α-cyano-4-hydroxycinnamic acid as matrix. Stock solutions of peptides were prepared by dissolving the peptide either in water or in 15% acetic acid. The concentrations of peptides were determined by monitoring absorbance at 280 nm.

Preparation of Small Unilamellar Vesicles (SUV)

Appropriate amounts of the lipids from stock solutions were mixed in chloroform/methanol to obtain the desired lipid composition and then dried using a rotavapor to obtain a thin lipid film. It was subjected to desiccation for 5–6 h. The lipid film was subsequently hydrated with 5 m*M* HEPES (pH 7.4) overnight. The suspension was sonicated until a clear solution was obtained. Titanium debris were removed by centrifugation.

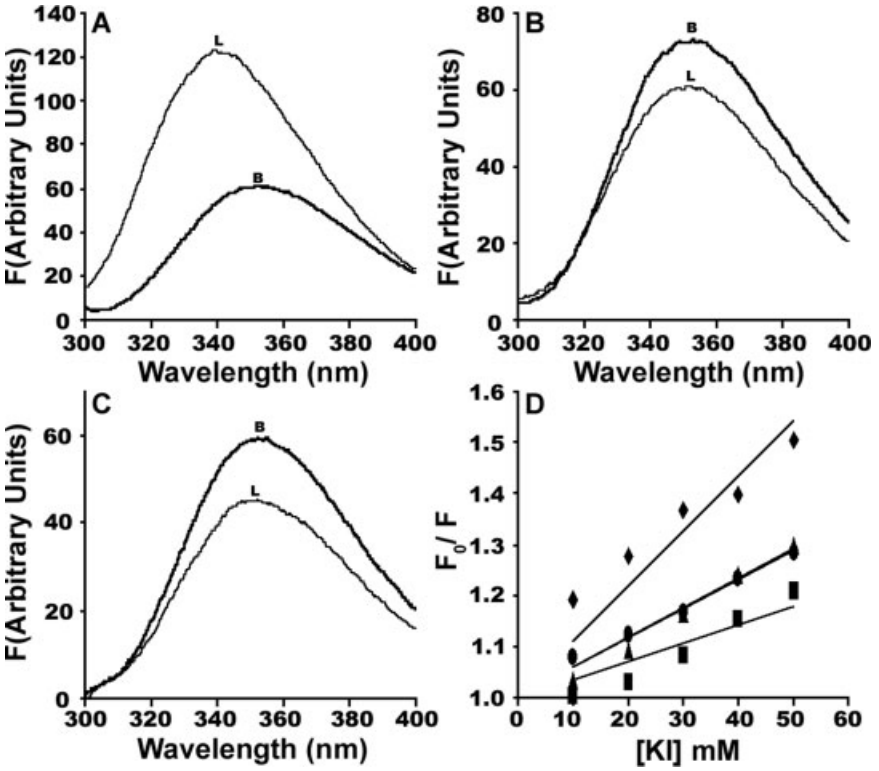

FIGURE 1 Fluorescence emission spectra of CSD AR in buffer, in the presence of lipid vesicles and quenching of tryptophan fluorescence by iodide. B denotes buffer and L denotes lipid vesicles. (A) PC : PG (1:1) (B) PC (C) PC : PE : SM : CHL (1:1:1:1.5). The data presented are maximal changes observed at lipid : peptide ratios = 70:1. (D) Stern–Volmer plots. Buffer (◆), PC : PG (▲), PC (■), PC : PE : SM : CHL (●).

Interaction with Lipid Vesicles

Emission spectra were recorded between 300 and 400 nm, with an excitation wavelength of 280 or 290 nm. The excitation and emission bandwidths were 5 nm. Lipid–peptide interactions were studied by monitoring the changes in Trp fluorescence spectra of the peptide upon titration with SUV with lipid compositions : PC, PC : PG (1:1), PC : PE : SM : CHL (1:1:1:1.5). Intrinsic fluorescence of Trp residues of the caveolin peptides and their variants was measured before and after addition of different amounts of lipid vesicles to 1 μM peptide solution. The same concentration of SUV without peptide was used as blank. All measurements were made on F4500 Hitachi fluorescence spectrometer (Hitachi, Tokyo, Japan). Solvent accessibility of the Trp residues in the peptides and their variants was assessed by monitoring quenching of fluorescence by I^- in the absence and presence of SUV (100 μM lipids), by addition of increasing amounts of 4 M KI solution containing 1 mM $Na_2S_2O_3$. The concentration of the peptide was 1 μM. The data were analyzed by Stern–Volmer plots using the equation $F_0/F = 1 + K_{sv}[Q]$, where F_0 and F are the fluorescence intensities of Trp in the absence and presence of quencher at concentration $[Q]$ respectively. K_{sv} is the Stern–Volmer quenching constant. The normalized accessibility factor (naf) was calculated from the ratios of K_{sv} obtained from the quenching of the Trp fluorescence in the presence and absence of liposomes.

Fluorescence resonance energy transfer (FRET) from the Trp residue to the DNS chromophore was determined by setting the excitation monochromator at 280 nm and monitoring the fluorescence emission between 300 and 550 nm. Lipid vesicles were doped with 2 mol % of DNS-PE. Peptides were titrated with labeled lipid vesicles and unlabeled lipid vesicles were added at the lowest lipid-to-peptide ratio. Changes in fluorescence were recorded after 15 min of incubation.

Gel filtration experiments were carried out as follows: peptides and SUV were mixed at varying lipid-to-peptide ratios. After recording the emission spectra, the SUV with bound peptide were gel filtered using Sephadex G-50. Fractions containing the liposome population were identified by 90° light scatter in a Hitachi F-4500 fluorescence spectrometer.

Hydrogen–Deuterium Exchange

Hydrogen–deuterium exchange was initiated by diluting peptide and peptide bound to lipid vesicles (peptide 3 μM; lipid 100 μM) in D_2O. MALDI spectra were recorded in reflectron mode after 3 h of H–D exchange on a Voyager DE STR mass spectrometer (Foster City, CA USA) using

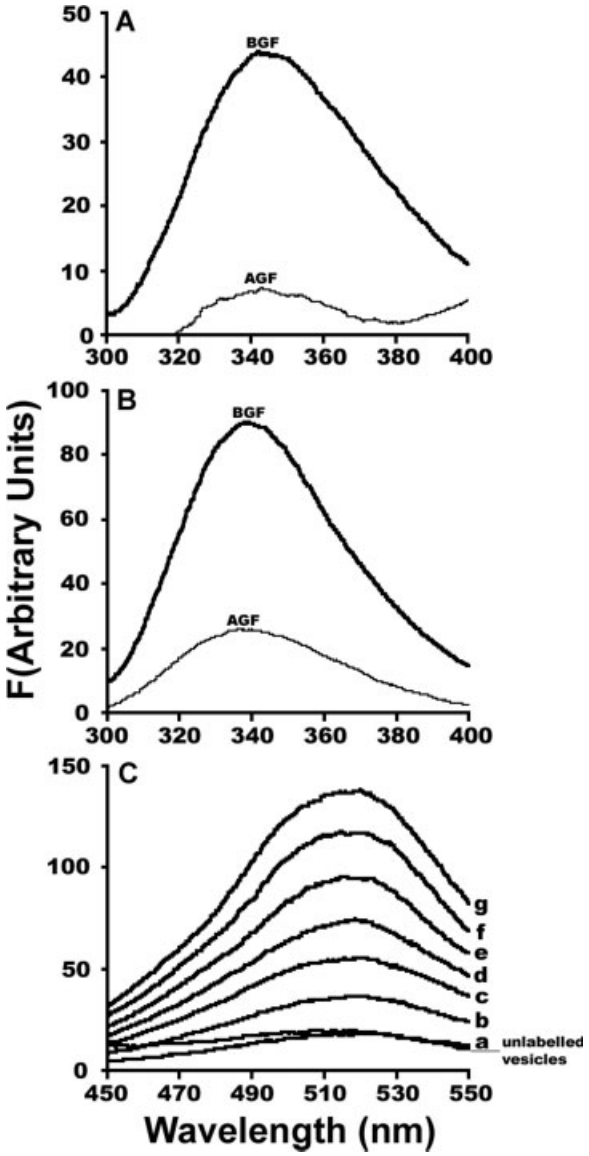

FIGURE 2 Interaction of CSD AR with lipid vesicles examined by gel filtration and fluorescence resonance energy transfer. BGF and AGF indicate fluorescence spectra in the presence of lipid vesicles before and after gel filtration, respectively. (A) PC, (B) PC : PG (1:1). (C) Fluorescence spectra of the DNS fluorophore upon addition of various concentrations (μM) of CSD AR (a,1; b,1.5; c, 2; d, 2.5; e, 3; f, 3.5; g, 4) to DNS-PE doped lipid vesicles. After the spectrum denoted by g was recorded, PC : PG vesicles without DNS-PE (800 μM) was added. The spectrum obtained after this addition is denoted as unlabeled vesicles.

recrystallized deuterated α-cyano-4-hydroxycinnamic acid as matrix. Average masses are the intensity-weighted average calculated from the sum of the fractional mass of each isotope as given by the following equation: Σ (mass $\times$ intensity of peak)/Σ (intensity of total isotopic peaks).

Circular Dichroism (CD)

CD measurements were carried out at 25°C on a JASCO J-715 spectropolarimeter (Jasco, Tokyo, Japan) between 195 and 250 nm in quartz cell with a path length of 1 mm. Data are represented as mean residue ellipticities. Spectra were recorded in water, TFE, and micelles of sodium dodecylsulfate (10 m*M*).

RESULTS

The aromatic amino acid–rich segment KYWFYR that occurs at the C-terminal of CSD of caveolin-1 is also present in the CSD of caveolin-3 except for the presence of cysteine instead of phenylalanine. We

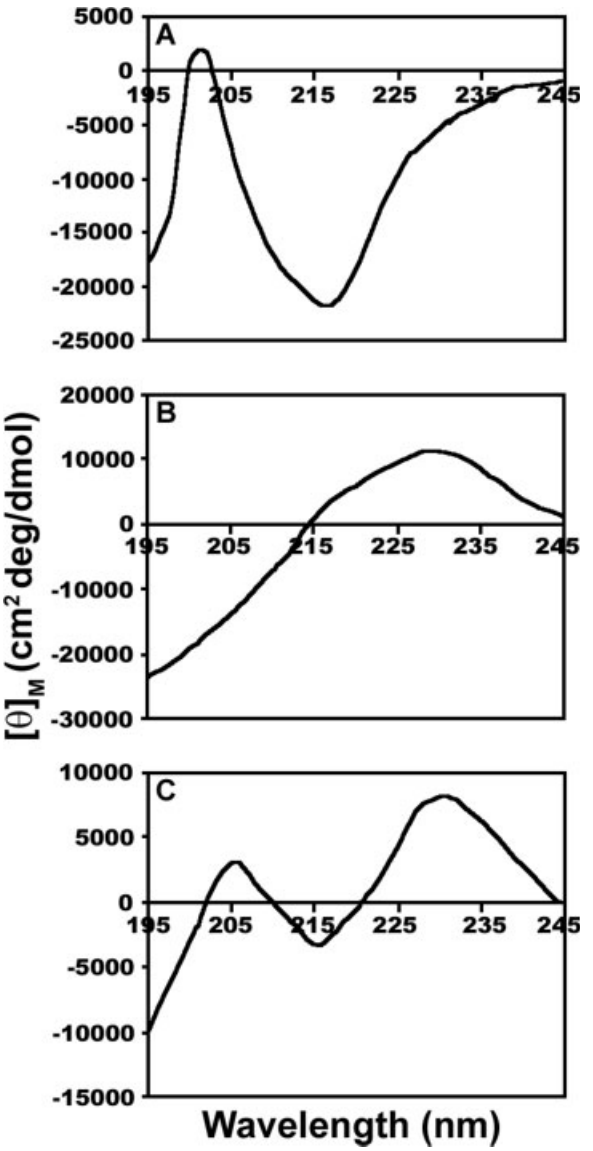

FIGURE 3 CD spectra of CSD AR. (A) Water, (B) TFE, (C) SDS. Peptide concentration was 30 μM in SDS and 10 μM in water and TFE.

have replaced the cysteine residue by phenylalanine. Although point mutations in caveolin-3 have been observed in limb girdle muscular dystrophy,[28–32] it is unlikely that this change will alter the properties of caveolin-3, as the cysteine→tryptophan change results in targeting of caveolin-3 to the plasma membrane.[31] The interaction of CSD AR (see Table I) with model membranes was examined by monitoring Trp fluorescence of the peptide. The location of Trp in the lipid bilayer was assessed by examining the quenching of Trp fluorescence by I^-. The data are shown in Figure 1A–D. The fluorescence spectra in the presence of lipids are those at which maximal changes were observed. Blue shift in λ_{max} and enhancement in intensity is observed in the presence of anionic PC : PG vesicles (Figure 1A). In the presence of PC and PC : PE : SM : CHL vesicles, there is no shift in the λ_{max}. There is also a decrease in intensity (Figure 1B and C). Despite minimal changes in the fluorescence properties, the Stern–Volmer plots (Figure 1D) indicate shielding of Trp from I^- in the presence of lipid vesicles.

The binding of CSD AR to lipid vesicles was further examined by gel filtration. Fluorescence spectra after gel filtration are shown in Figure 2A and B. The fluorescence spectrum characteristic of Trp was observed only in PC : PG vesicles (Figure 2B). When FRET between Trp and DNS fluorophore in PC : PG vesicles doped with DNS-PE was examined, considerable FRET is observed (Figure 2C). When challenged with unlabeled vesicles, the FRET decreased considerably (spectrum denoted unlabeled), indicating that the peptide is located at the bilayer surface.

The conformation of CSD AR was examined by CD and MALDI mass spectrometry. The CD spectrum shown in Figure 3A suggests β-structure in water. In TFE and micelles of SDS (Figure 3B and C), although the contributions from the aromatic residues complicate interpretation, the spectrum in SDS micelles suggests β-structure. The total number of exchangeable protons in CSD AR is 16, which include 5 backbone amide protons. The exchange behavior of protons with deuterium in D_2O was examined as a function of time. The MALDI mass spectra are shown in Figure 4. The isotopic distribution and the average mass of 973.76 [average mass in H_2O = 963.4 (Figure 4A)] indicate exchange of 10 protons (Figure 4B). In the presence of PC and PC : PE : SM : CHL vesicles, the isotopic distribution and the average mass values (967.11, Figure 4C; 969.13, Figure 4D) indicate that only 4 to 6 protons exchange with deuterium at this time, indicating that several protons are shielded from water in the presence of lipid vesicles.

The emission spectra of CSD19 and 16 in the presence of lipid vesicles are shown in Figure 5. Blue

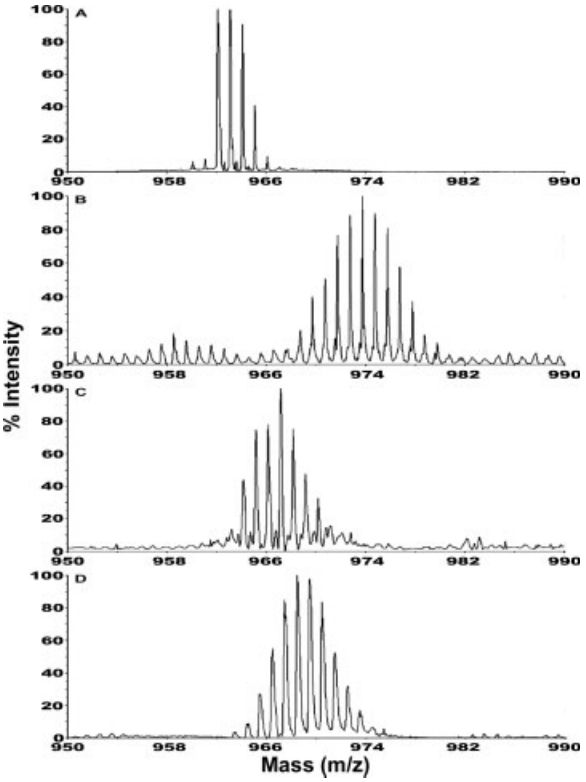

FIGURE 4 MALDI mass spectra of CSD AR under various conditions. (A) Water, (B) D_2O, (C) peptide bound to PC vesicles diluted 50-fold in D_2O, (D) peptide bound to PC : PE : SM : CHL vesicles diluted 50-fold in D_2O. Spectra were recorded 3 h after initiating H–D exchange. Lipid : peptide = 33:1.

shift in the λ_{max} and enhancement in intensity is observed in the presence of PC : PG (Figure 5A and D) and PC (Figure 5B and E) vesicles but not in the presence of PC : PE : SM : CHL vesicles (Figure 5C and F). The spectra shown are maximal changes observed at peptide-to-lipid ratios of 1:70. To examine how CSD AR modulates the interaction of the CSD or CSD with the TFT deletion with model membranes, the interaction of CSD15-AR and CSD12-AR with lipid vesicles is examined (see Figure 6). In the presence of PC : PG vesicles, only blue shift but no enhancement in intensity is observed (Figure 6A and D). The blue shift in λ_{max} and fluorescence intensity was much less in the presence of PC and PC : PE : SM : CHL vesicles (Figure 6B, C, E, and F).

The accessibility of Trp to I^- in CSD19, CSD16, CSD15-AR, and CSD12-AR in buffer and lipid vesicles was examined (see Figure 7). Although the emission spectra do not show drastic changes, shielding from the aqueous quenchers is evident for peptides (Figure 7A–C) with the exception of CSD12-AR (Figure 7D). The naf values for the five peptides cor-

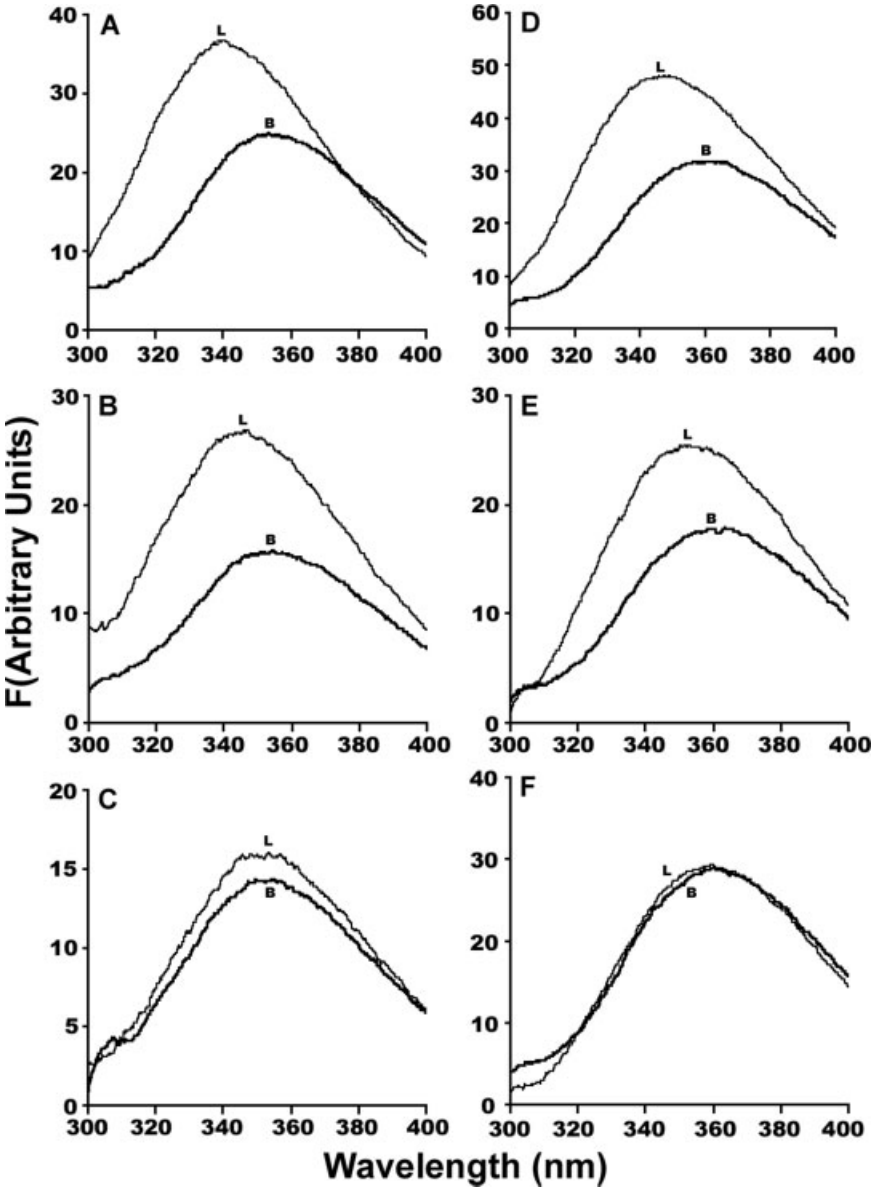

FIGURE 5 Fluorescence emission spectra of peptides in buffer and lipid vesicles. The spectra in buffer and lipid vesicles are indicated as B and L, respectively, near the traces. CSD19: (A) PC : PG, (B) PC, (C) PC : PE : SM : CHL. CSD16: (D) PC : PG, (E) PC, (F) PC : PE : SM : CHL. The data presented are maximal changes observed at lipid : peptide ratios = 70:1.

responding to various regions of CSD are compared in Figure 7E. In CSD AR, the Trp residue is more accessible to I^- when associated with PC : PG and SM-containing vesicles compared with PC. In CSD19 and CSD16, which have two Trp residues, accessibility to I^- is greater in SM-containing vesicles. In CSD16, which has the TFT deletion, the accessibility of Trp is less compared with CSD19 and minimum quenching is observed in PC : PG vesicles. In CSD15-AR, which has only one Trp, the quenching by I^- is comparable in all three vesicles. The quenching in SM-containing vesicles is less than in CSD AR and CSD19. Deletion of YWFYR does not prevent binding of the remaining segment of the CSD to membranes but further deletion of TFT decreases binding to PC and PC : PG vesicles considerably. The location of Trp in CSD12-AR and CSD AR appears to be similar in SM-containing vesicles.

The CD spectra of CSD15-AR and CSD12-AR in aqueous medium were characteristic of unordered conformation. In TFE, the spectra (Figure 8A and C) suggest a population of helical and unordered confor-

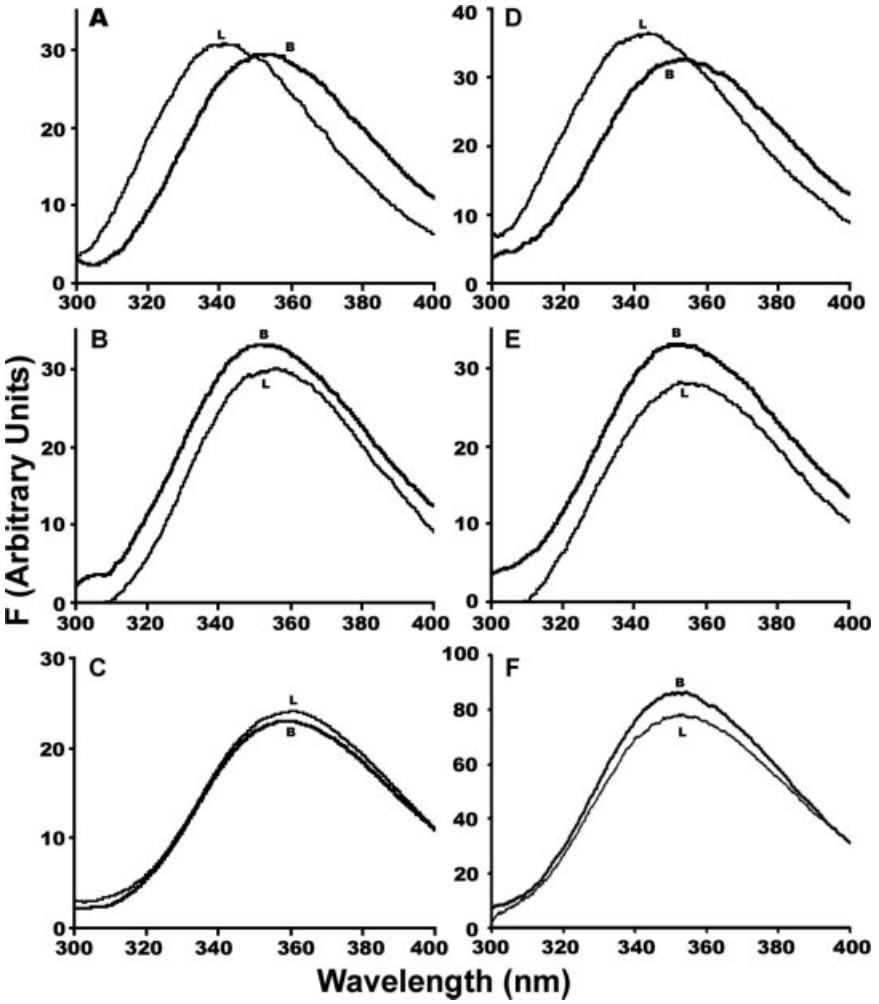

FIGURE 6 Fluorescence emission spectra of peptides in buffer and lipid vesicles. The spectra in buffer and lipid vesicles are indicated as B and L, respectively, near the traces. CSD15-AR: (A) PC : PG, (B) PC, (C) PC : PE : SM : CHL. CSD12-AR: (D) PC : PG, (E) PC, (F) PC : PE : SM : CHL. The data presented are maximal changes observed at lipid : peptide ratios = 70:1.

mation for both of the peptides. In SDS, the spectra of both of the peptides are characterized by a single negative minimum (Figure 8B and D). While a positive band is observed for CSD15-AR, it is absent in CSD12-AR. The spectra suggest that the peptides populate β-structure in a micellar environment.

DISCUSSION

The CSD of caveolins-1 and -3 have membrane-attachment properties.[23–26,32] Even the sequence KYWFYR, which occurs at the end of the CSD (Table I), appears to target a soluble protein to membranes in cells.[26] In caveolin-3, the microdeletion of TFT in the CSD leads to retention of the protein in the Golgi and increased detergent solubility.[30] We have examined the association of peptides corresponding to various regions of CSD of caveolin-3, to get an insight into how this segment, whose sequence is not typical of membrane-interacting sequences,[35] modulates the association of caveolin-3 with membranes. Our results show that the aromatic segment KYWFYR associates with zwitterionic, anionic, and sphingomyelin containing lipid vesicles, as evident from the gel filtration experiments and shielding of Trp from I^- when bound to lipids. Several protons in the peptides show slow exchange rates with deuterium in the presence of lipid vesicles, which we attribute to hydrogen bonding with polar atoms in the head group region. No specificity toward cholesterol-containing lipid vesicles was observed. It has been demonstrated by ^{1}H magic angle spinning nuclear overhauser effect spectroscopy that the CSD AR

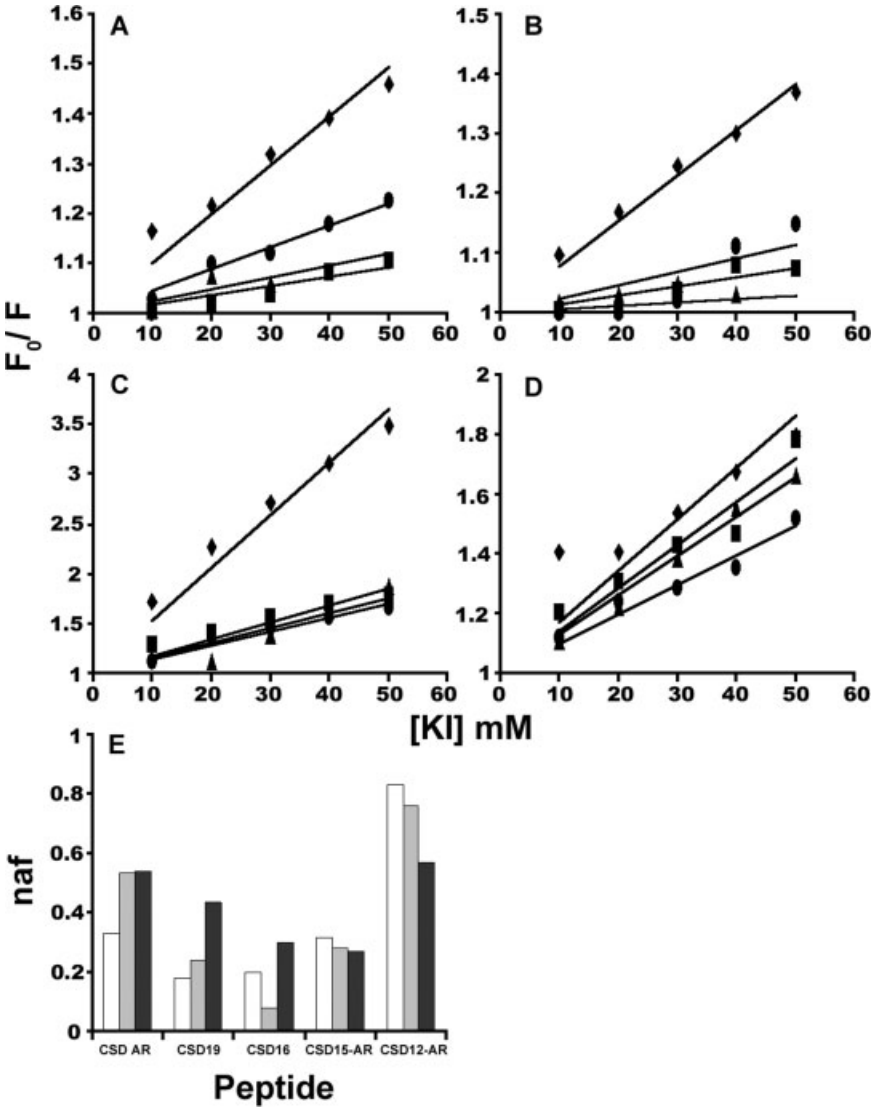

FIGURE 7 Quenching of tryptophan fluorescence in peptides by I^-. Stern–Volmer plots: (A), CSD19, (B) CSD16, (C) CSD15-AR, (D) CSD12-AR. Designations are: buffer (◆), PC : PG (▲), PC (■), PC : PE : SM : CHL (●). (E) Net accessibility factor in the presence of PC (white), PC : PG (1:1) (gray), PC : PE : SM : CHL (black).

sequence, acetylated at the N-terminus and amidated at the C-terminus, though it has the ability to bind to lipid vesicles, does not promote the formation of cholesterol crystallites or interact preferentially with cholesterol.[36,37]

All of the peptides corresponding to the CSD sequence of caveolin-3 appear to be peripherally bound on the bilayer surface with the Trp located near the ester bond region. The CSD of caveolin-1 induced the formation of membrane domains enriched in acidic lipids such as PS and PIP_2 in giant unilamellar vesicles.[38] Recombinant caveolin-1 incorporated to a much greater extent ($\sim$25- to 30-fold) in cholesterol-containing choline vesicles at a molar ratio of 1:1 compared with vesicles in the absence of cholesterol.[39] Such preferential incorporation into lipid vesicles containing sphingomyelin and 33 mol % cholesterol was not observed with peptides corresponding to CSD of caveolin-3. Hence, it appears that the CSD19 sequence in isolation does not have affinity for cholesterol-containing lipid vesicles. The peptides CSD19 and CSD16 do not have arginine (at the C-terminus), which occurs at the 74th position of human caveolin-3. As a result, these sequences would not have the cholesterol recognition/interaction consensus (CRAC) motif.[40,41] Although CSD AR has an arginine residue at the C-terminus, the sequence does not correspond to the CRAC motif. Hence, it

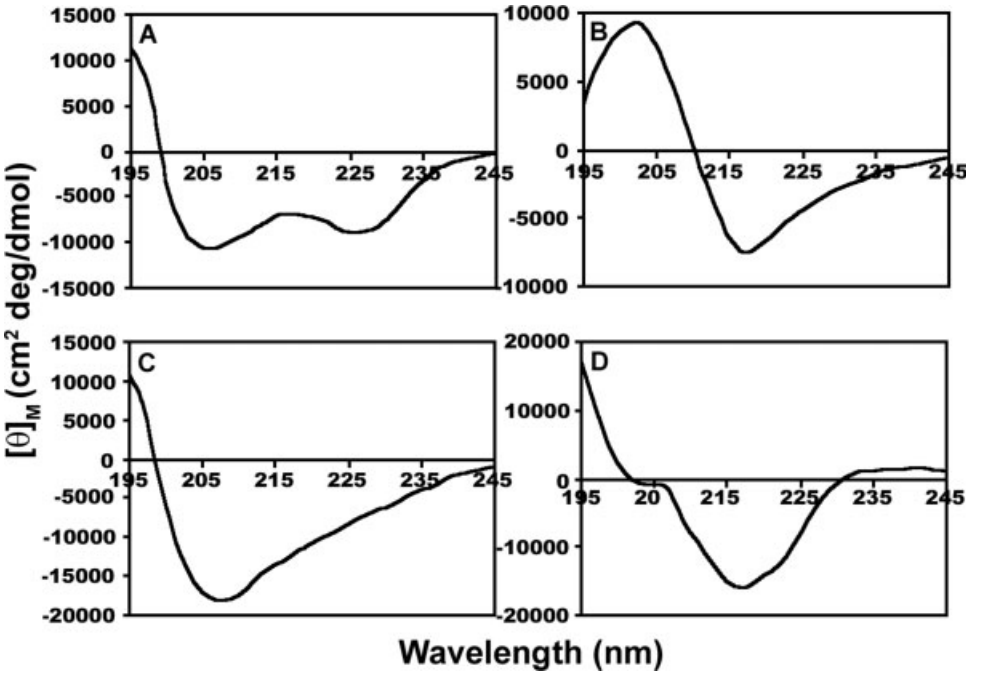

FIGURE 8 CD spectra of peptides. CSD15-AR: (A) TFE, (B) SDS. CSD12-AR: (C) TFE, (D) SDS. Peptide concentrations were 30 μM except for CSD15-AR in TFE, for which the concentration was 10 μM.

may be argued that these peptides do not show preferential binding to cholesterol-containing vesicles. However, even peptides corresponding to the CSD of caveolin-1, which have the CRAC motif, though they had the ability to promote segregation of cholesterol into domains in vesicles containing 40 mol % cholesterol, were less selective in binding to cholesterol domains compared with a short 5-residue peptide having the CRAC motif.[37] Relatively small changes in the emission spectra of Trp in the absence and presence of lipid vesicles containing cholesterol were also observed in these peptides corresponding to the CSD of caveolin-1[37] and the peptides appeared to be localized peripherally on the bilayer surface of POPC vesicles.[37,42] It has been argued that the interaction of peptides corresponding to the CSD of caveolin-1 with cholesterol, which have the CRAC motif, is not likely to be specific.[37] The cholesterol requirement observed in caveolin-1 may be necessary for the association of the transmembrane and C-terminal membrane-attachment domain with membranes. The naf values do show differences in CSD AR and CSD19 in the presence of PC vesicles with and without cholesterol. The Trp residues appear to be more accessible to I^- in cholesterol-containing vesicles. This is less apparent when the sequence TFT or YWFYR is deleted from the CSD19. The absence of intimate association of the CSD with the lipid bilayer would facilitate interaction with other proteins in the signaling pathways. Also, CSD is part of the oligomerization domain of caveolin-1 and -3.[7,10,23] For these multipurpose functions, strong membrane association of the CSD may not be desirable.

Deletion of the sequence WFYR from the CSD of caveolin-1 resulted in the passenger protein equally distributed between soluble and membrane fractions,[26] suggesting that the CSD without this segment may have lower affinity for membranes. Since the CSD of caveolin-1 and -3 have a high degree of homology and are functionally similar, it is likely that a similar effect would have been observed with caveolin-3. Our results indicate that CSD15-AR does associate with lipid vesicles. However, the difference in the accessibility of Trp to the aqueous quencher I^-, as observed in CSD19 with different lipids, is absent. It is also possible that the tryptophans in the CSD15-AR segment and KYWFYR have different orientations on the bilayer surface. This could arise because of differences in the conformational propensities between the peptides with[43] and without the AR segment in a membrane-mimicking environment such as SDS micelles. Caveolin-3 mutants have been transiently expressed in NIH 3T3 cells. When membrane fractions were analyzed, caveolin-3 with TFT deletion was significantly more Triton X-100 soluble compared with wild-type caveolin-3.[30] The TFT dele-

tion also affected the oligomerization of caveolin-3, leading to formation of unstable high molecular mass aggregates that were retained within the Golgi complex.[30] Our results indicate that deletion of TFT from the CSD of caveolin-3 does have an effect on the association of the peptide with lipid vesicles compared with the wild-type sequence, particularly with lipid vesicles composed of PC : PG. Affinity for lipids decreases considerably when TFT and YWFYR are deleted from the CSD sequence. Thus, in addition to subtle changes in conformation,[43] deletion of TFT does modulate association of the CSD segment of caveolin-3 with lipid membranes.

REFERENCES

1. Palade, G. E. J Appl Phys 1953, 24, 1424.
2. Yamada, E. J Biophys Biochem Cytol 1955, 1, 445–458.
3. Carver, L. A.; Schnitzer, J. E. Nat Rev Cancer 2003, 3, 571–581.
4. Galbiati, F.; Razani, B.; Lisanti M. P. Cell 2001, 106, 403–411.
5. Parton, R. G. Curr Opin Cell Biol 1996, 8, 542–548.
6. Razani, B.; Lisanti, M. P. Exp Cell Res 2001, 271, 36–44.
7. Razani, B.; Woodman, S. E.; Lisanti, M. P. Pharmacol. Rev 2002, 54, 431–467.
8. van Deurs, B.; Roepstorff, K.; Hommelgaard, A. M.; Sandvig, K. Trends Cell Biol 2003, 13, 92–100.
9. Williams, T. M.; Lisanti, M. P. Am J Physiol. Cell Physiol 2005, 288, C494–C506.
10. Liu, P.; Rudick, M.; Anderson, R. G. W. J Biol. Chem. 2002, 277, 41295–41298.
11. Okamoto, T.; Schlegel, A.; Scherer, P. E.; Lisanti, M. P. J Biol Chem 1998, 273, 5419–5422.
12. Razani, B.; Schlegel, A.; Lisanti, M. P. J Cell Sci 2000, 113, 2103–2109.
13. Smart, E. J.; Graf, G. A.; McNiven, M. A.; Sessa, W. C.; Engelman, J. A.; Scherer, P. E.; Okamoto, T.; Lisanti, M. P. Mol Cell Biol 1999, 19, 7289–7304.
14. Williams, T. M.; Lisanti, M. P. Genome Biol. 2004, 5, 214.1–214.8.
15. Scherer, P. E.; Okamoto, T.; Chun, M.; Nishimoto, I.; Lodish, H. F.; Lisanti, M. P. Proc Natl Acad Sci U S A 1996, 93, 131–135.
16. Scherer, P. E.; Lewis, R. Y.; Volonte, D.; Engelman, J. A.; Galbiati, F.; Couet, J.; Kohtz, D. S.; van Donselaar, E.; Peters, P.; Lisanti, M. P. J Biol Chem 1997, 272, 29337–29346.
17. Song, K. S.; Scherer, P. E.; Tang, Z.; Okamoto, T.; Li, S.; Chafel, M.; Chu, C.; Kohtz, D. S.; Lisanti, M. P. J Biol Chem 1996, 271, 15160–15165.
18. Tang, Z.; Scherer, P. E.; Okamoto, T.; Song, K.; Chu, C.; Kohtz, D. S.; Nishimoto, I.; Lodish, H. F.; Lisanti, M. P. J. Biol. Chem. 1996, 271, 2255–2261.
19. Monier, S.; Parton, R. G.; Vogel, F.; Behlke, J.; Henske, A.; Kurzchalia, T. V. Mol Biol Cell 1995, 6, 911–927.
20. Sargiacomo, M.; Scherer, P. E.; Tang, Z.; Kubler, E.; Song, K. S.; Sanders, M. C.; Lisanti, M. P. Proc Natl Acad Sci U S A 1995, 92, 9407–9411.
21. Das, K.; Lewis, R. Y.; Scherer, P. E.; Lisanti, M. P. J Biol Chem 1999, 274, 18721–18728.
22. Li, S.; Couet, J.; Lisanti, M. P. J Biol Chem 1996, 271, 29182–29190.
23. Machleidt, T.; Li, W. P.; Liu, P.; Anderson, R. G. W. J Cell Biol 2000, 148, 17–28.
24. Schlegel, A.; Schwab, R. B.; Scherer, P. E.; Lisanti, M. P. J Biol Chem 1999, 274, 22660–22667.
25. Schlegel, A.; Lisanti, M. P. J Biol Chem 2000, 275, 21605–21617.
26. Woodman, S. E.; Schlegel, A.; Cohen, A. W.; Lisanti, M. P. Biochemistry 2002, 41, 3790–3795.
27. Dupree, P.; Parton, R. J.; Raposo, G.; Kurzchalia, T. V.; Simons, K. EMBO J 1993, 12, 1597–1605.
28. McNally, E. M.; de Sa Moreiraqq, E.; Duggan, D. J.; Bonnemann, C. G.; Lisanti, M. P.; Lidov, H. G. W.; Vainzof, M.; Passos-Bueno, M. R.; Hoffman, E. P.; Zatz, M.; KunKel, L. M. Hum Mol Genet 1998, 7, 871–877.
29. Minetti, C.; Sotgia, F.; Bruno, C.; Scartezzini, P.; Broda, P.; Bado, M.; Masetti, E.; Mazzocco, M.; Egeo, A.; Donati, M. A.; Volonte, D.; Galbiati, F.; Cordone, G.; Bricarelli, F. D.; Lisanti, M. P.; Zara, F. Nat Genet 1998, 18, 365–368.
30. Galbiati, F.; Volonte, D.; Minetti, C.; Chu, J. B.; Lisanti, M. P. J Biol Chem 1999, 274, 25632–25641.
31. Carozzi, A. J.; Roy, S.; Morrow, I. C.; Pol, A.; Wyse, B.; Clyde-Smith, J.; Prior, Nixon, S. J.; Hancock, J. F.; Parton, R. G. J Biol Chem 2002, 277, 17944–17949.
32. Smythe, G. M.; Eby, J. C.; Disatnik, M. H.; Rando, T. A. J Cell Sci 2003, 116, 4739–4749.
33. Atherton, E.; Sheppard, R. C. Solid Phase Peptide Synthesis: A Practical Approach. IRL Press: Oxford 1989.
34. Guy, C. A.; Fields, G. B. Methods Enzymol. 1997, 289, 67–83.
35. Popot, J. L.; Engelman, D. M. Annu Rev Biochem 2000, 69, 881–922.
36. Epand, R. M.; Sayer, B. G.; Epand, R. F. Biochemistry 2003, 42, 14677–14689.
37. Epand, R. M.; Sayer, B. G.; Epand, R. F. J Mol Biol 2005, 345, 339–350.
38. Wanaski, S. P.; Ng, B. K.; Glaser, M. Biochemistry 2003, 42, 42–56.
39. Li, S.; Song, K. S.; Lisanti, M. P. J Biol Chem 1996, 271, 568–573.
40. Li, H.; Papadopoulos, V. Endocrinology 1998, 139, 4991–4997.
41. Li, H.; Yao, Z.; Degenhardt, B.; Teper, G.; Papadopoulos, V. Proc Natl Acad Sci U S A 2001, 98, 1267–1272.
42. Arbuzova, A.; Wang, L.; Wang, J.; Hangyas-Mihalyne, G.; Murray, D.; Honig, B.; McLaughlin, S. Biochemistry 2000, 39, 10330–10339.
43. Jagannadham, M. V.; Sharadadevi, A.; Nagaraj, R. Biochem. Biophys Res Commun 2002, 298, 203–206.